

## Enhanced Water Oxidation on $Ta_3N_5$ Photocatalysts by Modification with Alkaline Metal Salts

Su Su Khine Ma,<sup>†</sup> Takashi Hisatomi,<sup>†</sup> Kazuhiko Maeda,<sup>†,‡,‡</sup> Yosuke Moriya,<sup>†</sup> and Kazunari Domen\*,<sup>†</sup>

<sup>†</sup>Department of Chemical System Engineering, The University of Tokyo, 7-3-1 Hongo, Bunkyo-ku, Tokyo 113-8656, Japan

<sup>‡</sup>Precursory Research for Embryonic Science and Technology (PRESTO), Japan Science and Technology Agency (JST), 4-1-8 Honcho Kawaguchi, Saitama 332-0012, Japan

### Supporting Information

**ABSTRACT:** Tantalum nitride ( $Ta_3N_5$ ) is a promising nitride semiconductor photocatalyst for solar water splitting because it has band edge potentials capable of producing hydrogen and oxygen from water under visible light ( $\lambda < 590$  nm). However, the photocatalytic performance of  $Ta_3N_5$  has been far below expectations because insufficient crystallization upon thermal nitridation of the oxide precursors enhances undesirable charge recombination limiting the quantum efficiency of the photocatalytic reaction. This problem was successfully rectified in this study by modifying the surface of the starting  $Ta_2O_5$  with a small amount of alkaline metal (AM) salts. Compared with conventional  $Ta_3N_5$ ,  $Ta_3N_5$  nitrided from AM salt-modified  $Ta_2O_5$  had better crystallinity and smaller particles with smoother surfaces and, most importantly, demonstrated a 6-fold improvement in photocatalytic activity for  $O_2$  evolution under visible light. AM salt modification was compatible with the loading of an  $O_2$  evolution cocatalyst, such as  $CoO_x$ , yielding an apparent quantum efficiency of 5.2% at 500–600 nm. This indicates that the effects of AM modification were attributable to the changes in the crystallinity and the morphology of  $Ta_3N_5$  rather than to catalytic effects. Detailed characterization of the  $Na_2CO_3$ -modified  $Ta_3N_5$  suggested partial dissolution of  $Ta_2O_5$  and nucleation of  $NaTaO_3$  in the early stages of nitridation, which gave rise to the characteristic particle morphologies and improved the crystallinity of the nitridation products. This study demonstrates that a facile pretreatment of a starting material can improve the physical and photocatalytic properties of photocatalysts drastically, enabling the development of advanced photocatalysts for solar water splitting.

reported that  $Ta_3N_5$  generates hydrogen or oxygen from water under visible light in the presence of a sacrificial electron donor or acceptor, respectively.<sup>2</sup>  $Ta_3N_5$  can also be applied as an  $O_2$  evolution photocatalyst and as a photoanode for Z-scheme<sup>5</sup> and photoelectrochemical water splitting<sup>6</sup> respectively. Comparing the two half-reactions of overall water splitting, oxygen generation is considered to be kinetically more challenging than hydrogen generation.<sup>7,8</sup> It is therefore important to address this issue through the development of innovative strategies to enhance the photocatalytic activity of candidate materials for  $O_2$  evolution. Besides cocatalyst loading to boost  $O_2$  evolution kinetics, doping and various synthesis methods involving flux treatments have been investigated to improve the inherent physical properties of semiconductor photocatalysts.<sup>9–14</sup> In general, doping has been found to have positive effects in four main areas: structural,<sup>9</sup> electronic,<sup>10</sup> optical,<sup>11</sup> and morphological.<sup>12</sup> Flux treatments during and after the synthesis of photocatalytic materials have been reported to alter both morphological and crystallographic aspects.<sup>13a</sup>

To tailor the morphology and improve the photocatalytic performance of  $Ta_3N_5$ , a flux was utilized in the synthesis of  $Ta_3N_5$ .<sup>13a</sup> It was also reported that, through doping with alkaline metal (AM) ions, the photoelectrochemical performance of nanostructured  $Ta_3N_5$  in water oxidation could be enhanced because of tunable band gaps and an enhancement of the electrode conductivity.<sup>14</sup> However, such positive effects are often overwhelmed by the detrimental effects of flux and dopants residues, such as decreased crystallinity and higher trap site densities, especially in photocatalytic  $O_2$  evolution reactions where both reduction and oxidation reactions take place on the surface of  $Ta_3N_5$  unlike photoelectrochemical reactions. In fact, reports in which the photocatalytic activity of  $Ta_3N_5$  was actually improved by modifiers, such as a flux, or dopants are rare, indicating that innovative and controllable methods are still needed to take advantage of the favorable effects of modifiers.

We report facile modification of  $Ta_2O_5$  with AM salts to produce a highly active  $Ta_3N_5$  photocatalyst for water oxidation in an aqueous  $AgNO_3$  solution under visible light irradiation. Typically, AM salts and  $Ta_2O_5$  powder were mixed (AM/Ta = 0.1 by mole) and annealed in air at 773 K for 2 h. The AM-modified  $Ta_2O_5$  (AM/ $Ta_2O_5$ ) was then nitrided under  $NH_3$  flow (300 mL/min) at 1123 K for 20 h, yielding AM-modified  $Ta_3N_5$  (AM/ $Ta_3N_5$ ). In some cases, the obtained AM/ $Ta_3N_5$  was rinsed

**P**hotocatalytic water splitting may provide an economically viable approach to the direct conversion of solar energy into renewable and storable hydrogen and oxygen, since both water and sunlight are naturally abundant. Due to its simplicity, water splitting using a powdered photocatalyst has stimulated great interest, especially with a focus on visible light responsive photocatalysts for effective utilization of sunlight.<sup>1</sup> Tantalum nitride ( $Ta_3N_5$ ) is one of the most promising photocatalysts for solar energy conversion via water splitting because it has a band gap of 2.1 eV and suitable band edge positions.<sup>2–5</sup> It has been

**Received:** September 27, 2012

**Published:** November 26, 2012

**Table 1.** Physical Properties of AM Salt-Modified  $Ta_3N_5$ 

AM salt	crystallite size, nm <sup>a</sup>	BET surface area, m <sup>2</sup> g <sup>-1</sup>	surface composition <sup>b</sup>		bulk composition <sup>c</sup> N/(O+N)
			AM/Ta	N/Ta	
none ( $Ta_3N_5$ )	33 (32)	9.9 (10.1)	no data	0.15 (0.15)	0.96
NaCl	43 (43)	7.1 (6.3)	0.18 (0.00)	0.17 (0.17)	0.96
$Na_2CO_3$	46 (47)	5.7 (6.0)	0.40 (0.08)	0.15 (0.14)	0.94
KCl	33 (33)	8.0 (7.6)	0.04 (0.00)	0.16 (0.12)	0.95
$K_2CO_3$	45 (41)	5.0 (5.6)	0.10 (0.02)	0.18 (0.19)	0.94
LiCl	49 (50)	4.0 (4.5)	0.00 (0.00)	0.00 (0.00)	0.95
$Li_2CO_3$	51 (51)	3.4 (3.9)	0.20 (0.00)	0.15 (0.14)	0.95

<sup>a</sup>Estimated by Scherrer's equation. <sup>b</sup>Estimated by XPS. <sup>c</sup>Estimated by oxygen–nitrogen combustion analysis. Data in parentheses correspond to data obtained after washing with water.

thoroughly with water to remove AM salt residue. To obtain the highest activity,  $CoO_x$  (2 wt%) was loaded on AM/ $Ta_3N_5$  by impregnation using a  $Co(NO_3)_2 \cdot 6H_2O$  aqueous solution followed by annealing at 773 K for 1 h in an  $NH_3$  flow<sup>13b</sup> (see Supporting Information for experimental details).

All samples prepared with 10% AM salts exhibited single-phase XRD patterns associated with anatase-type  $Ta_3N_5$  (Figure S1A). Marginal peak shifts toward smaller diffraction angles suggested that the AM cations were not significantly incorporated into the  $Ta_3N_5$  lattice. This is because the AM salts employed were not small enough to replace  $Ta^{5+}$  ions fully but rather evaporated under the nitridation conditions. Sharper diffraction peaks, larger crystallite sizes, and smaller BET surface areas (Table 1) for AM/ $Ta_3N_5$  were indicative of higher sample crystallinity. As seen in the UV-vis diffuse reflectance spectra (DRS, Figure S1C), no noticeable change was observed in the absorption edge wavelengths among the synthesized AM/ $Ta_3N_5$  and conventional  $Ta_3N_5$  samples. Steep onset of light absorption at ~600 nm characteristic of  $Ta_3N_5$  is attributable to electron transitions from N 2p orbitals to empty Ta 5d orbitals.<sup>2</sup> Since the bulk nitrogen contents were almost identical regardless of the AM salt modification, it is reasonable that the band gap energies were unchanged.

Figures 1 and S2 show changes in the surface morphology of  $Ta_3N_5$  particles after modification with AM ions observed by

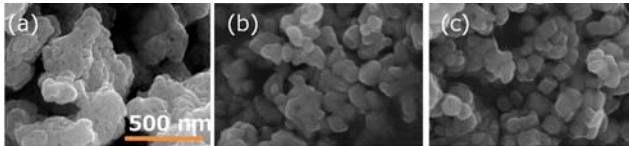


**Figure 1.** SEM images of  $Ta_3N_5$  prepared from  $Ta_2O_5$  (a) unmodified and modified with (b) NaCl and (c)  $Na_2CO_3$ .

SEM. The porous structure typical of unmodified  $Ta_3N_5$ <sup>13a</sup> disappeared with the AM salt modification. All of the AM/ $Ta_3N_5$  except Li salt/ $Ta_3N_5$  exhibited monodisperse fine particles ~80 nm on average in size, which was considerably smaller than the particle size of the starting  $Ta_2O_5$  and conventional  $Ta_3N_5$  (150–400 nm). This was due to surface dissolution of the  $Ta_3N_5$  particles and nucleation of alkali tantalate caused by the small

amount of AM salts, as discussed later. Larger particle sizes of Li salt/ $Ta_3N_5$  were probably due to the low melting points of LiCl (886 K) and  $Li_2CO_3$  (1005 K), and the relatively close ionic radii of the six-fold coordinated  $Li^+$  (90 pm) and  $Ta^{5+}$  (78 pm) ions, which would enable interdiffusion of the constituent cations and growth of Li salt/ $Ta_3N_5$  particles. Note that the particle sizes estimated by SEM observation were larger than the crystallite sizes presented in Table 1 owing to possible formation of secondary particles. As shown in Table 1, the AM/ $Ta_3N_5$  samples had lower specific surface areas than conventional  $Ta_3N_5$ . This is consistent with the lack of mesopores in the AM/ $Ta_3N_5$  particles, as observed in SEM images. Rinsing of AM/ $Ta_3N_5$  did not significantly change the XRD patterns, DRS, SEM images, or BET surface areas.

XPS of as-prepared  $Ta_3N_5$  modified with NaCl,  $Na_2CO_3$ , KCl,  $K_2CO_3$ , LiCl, or  $Li_2CO_3$  indicated the presence of the respective AM species on the surface, as shown in Table 1 and Figure S3C. After thorough washing with distilled water, signals from the AM species disappeared when chlorides were used as modifiers but not completely in the case of the carbonate modifiers. It is possible that the carbonates with higher basicity allowed for more intensive reaction with  $Ta_2O_5$  than the chlorides, so that some of the AM species could be incorporated into the surface of the AM/ $Ta_3N_5$ . However, it is likely that the incorporation of small amounts of AM species did not strongly affect the valence states of the Ta species. Binding energies of the Ta 4f peaks were 26.6 and 28.5 eV for all of the  $Ta_3N_5$ , whether unmodified or modified with AM salts (Figure S3A). In addition, the N 1s XPS peaked at 397 eV, indicating the formation of Ta–N bonds (Figure S3B). Nitrogen contents estimated by XPS are inevitably smaller than the chemical formula because of natural oxidation layers. However, as in Table 1, surfaces of all of the prepared samples had N/Ta ratios similar to that of conventional  $Ta_3N_5$ . This suggests that the surface composition was not affected significantly by the AM salt modification. In addition, O/N combustion analysis indicated that the decrease in nitrogen-to-anion ratio (N/(N+O)) after the incorporation of AM salts was ~2% (from 96 to 94%) at most. These results confirm that Ta species predominantly existed as  $Ta_3N_5$  and not as alkali tantalates, consistent with XRD analyses (Figure S1A) which did not indicate the presence of any crystalline impurities.

Photocatalytic  $O_2$  evolution activity of the prepared samples before and after washing is presented in Figure 2. All of the pristine AM/ $Ta_3N_5$  samples exhibited  $O_2$  evolution rates more than double those of the unmodified samples. However, after rinsing with distilled water, the activity of  $Ta_3N_5$  modified with

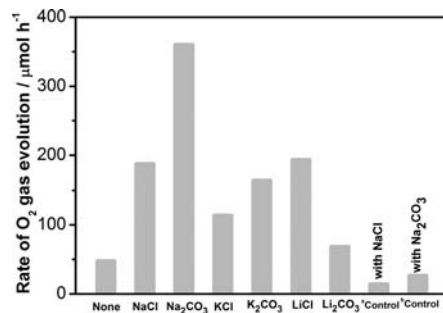


**Figure 2.** Rates of  $O_2$  evolution over AM/ $Ta_3N_5$  (AM/Ta = 0.1). Conditions: catalyst, 0.1 g; 50 mM aq  $AgNO_3$  solution, 100 mL, 0.1 g of  $Ta_2O_5$  as pH buffer; light source, 300 W xenon lamp ( $420 < \lambda < 800$  nm). <sup>a</sup>NaCl was added and <sup>b</sup> $Na_2CO_3$  was added (Na/Ta = 0.1).

chlorides decreased markedly. It is presumably because the surface of  $\text{Ta}_3\text{N}_5$  modified with chlorides would not be as crystalline as those modified with carbonates. As a result, they could undergo deactivation via dissolution of the surface during the rinsing. In fact, the crystallite sizes of AM/ $\text{Ta}_3\text{N}_5$  prepared from  $\text{NaCl}/\text{Ta}_2\text{O}_5$  and  $\text{KCl}/\text{Ta}_2\text{O}_5$  were slightly smaller than those prepared from  $\text{Na}_2\text{CO}_3/\text{Ta}_3\text{N}_5$  and  $\text{K}_2\text{CO}_3/\text{Ta}_3\text{N}_5$  (Table 1).

Since XPS analysis indicated the presence of AM residue on the surface, one might suspect that  $\text{AgCl}$  and  $\text{Ag}_2\text{O}$  originating from chloride and carbonate residue may have contributed to the higher activity of unwashed AM/ $\text{Ta}_3\text{N}_5$ . However, this possibility was excluded by the control photocatalytic reactions: when an equivalent amount of sodium chloride or carbonate was intentionally added into a reaction solution containing conventional  $\text{Ta}_3\text{N}_5$ , the  $\text{O}_2$  evolution rates decreased. Accordingly, it is reasonable to tentatively attribute the enhanced photocatalytic activity of AM/ $\text{Ta}_3\text{N}_5$  to changes in the physical properties of  $\text{Ta}_3\text{N}_5$ , such as particle morphology, crystallinity, and donor concentrations. However, it is highly unlikely that AM ions acted as a p-type dopant because, as in Figure S4, both unmodified and  $\text{Na}_2\text{CO}_3$  modified  $\text{Ta}_3\text{N}_5$  photoelectrodes generated anodic photocurrents characteristic of n-type semiconductivity.<sup>6,14</sup> Moreover, the onset potential of the transient anodic photocurrents under intermittent illumination did not shift positively by the  $\text{Na}_2\text{CO}_3$  modification, suggesting that the flat band potential was not affected significantly by the marginal incorporation of Na species in  $\text{Ta}_3\text{N}_5$ . It is reasonable to assume that the flat band potential of  $\text{Ta}_3\text{N}_5$  is largely governed by anion vacancies rather than small amounts of AM ions, since it is widely accepted that a number of anion vacancies are generated during nitridation reaction under high-temperature ammonia flow that is highly reductive.

The effect of the AM salt modification on  $\text{H}_2$  evolution activity was also investigated using  $\text{Pt}/\text{Ta}_3\text{N}_5$  and  $\text{Pt}/\text{Na}_2\text{CO}_3/\text{Ta}_3\text{N}_5$ . However, the impact of AM addition on the  $\text{H}_2$  evolution rate was not significant in preliminary trials. Since photocatalytic  $\text{H}_2$  evolution activity depends heavily on cocatalyst loading, refinement of modification methods of  $\text{Ta}_3\text{N}_5$  is necessary to discuss the effect of AM salt modification on the photocatalytic  $\text{H}_2$  evolution unambiguously.

Among the AM salt precursors examined,  $\text{Na}_2\text{CO}_3$  was found to be the most suitable for the preparation of highly active AM/ $\text{Ta}_3\text{N}_5$  for  $\text{O}_2$  evolution. Therefore, effects of  $\text{O}_2$  evolution cocatalysts were investigated using  $\text{Na}_2\text{CO}_3/\text{Ta}_3\text{N}_5$ . The dependence of  $\text{O}_2$  evolution rates on the cocatalysts loaded under various conditions is shown in Figure 3, and reaction time courses of representative samples are shown in Figure S5. Nitrogen evolution due to the oxidation of  $\text{Ta}_3\text{N}_5$  was suppressed or not detected after cocatalyst loading (Figure S5b).  $\text{Na}_2\text{CO}_3/\text{Ta}_3\text{N}_5$  samples loaded with 1 wt% Ir or 2 wt%  $\text{CoO}_x$  yielded higher  $\text{O}_2$  evolution activity than pristine  $\text{Na}_2\text{CO}_3/\text{Ta}_3\text{N}_5$ , although excessive cocatalyst loading and annealing at a high temperature led to lower performance. The highest activity was obtained with 2 wt% of  $\text{CoO}_x$  loading followed by  $\text{NH}_3$  treatment at 773 K for 1 h. Consequently, the  $\text{O}_2$  evolution rate of conventional  $\text{Ta}_3\text{N}_5$  increased from 55 to 450  $\mu\text{mol}/\text{h}$  after modification with  $\text{Na}_2\text{CO}_3$  and subsequent loading of the  $\text{CoO}_x$  cocatalyst, corresponding to apparent quantum efficiencies (AQYs) of 1.3 and 5.2% at 500–600 nm, respectively. The AQY of the  $\text{CoO}_x$  loaded  $\text{Na}_2\text{CO}_3/\text{Ta}_3\text{N}_5$  is one of the highest values ever reported at the long wavelength region, while higher

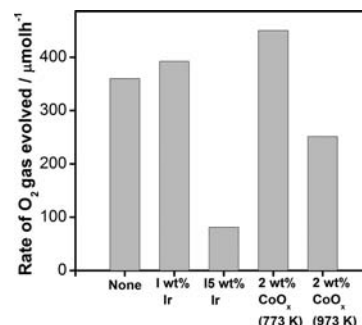


**Figure 3.** Rates of  $\text{O}_2$  evolution over  $\text{Na}_2\text{CO}_3$ -modified  $\text{Ta}_3\text{N}_5$  loaded with Ir or  $\text{CoO}_x$ . Conditions: catalyst, 0.1 g; 50 mM aqueous  $\text{AgNO}_3$  solution, 100 mL, 0.1 g of  $\text{La}_2\text{O}_3$  as pH buffer; light source, 300 W xenon lamp ( $420 < \lambda < 800 \text{ nm}$ ).

AQYs have been reported at shorter wavelengths for  $\text{BiVO}_4$  (9% at 450 nm)<sup>15</sup> and  $\text{LaTiO}_2\text{N}$  (27% at 440 nm).<sup>13b</sup>

Importantly, effects of AM salt modification and the catalytic enhancement by  $\text{CoO}_x$  loading were accumulative. Considering the structural features, photocatalytic activity, and photoelectrochemical properties together, it is reasonable to attribute the positive effects of AM salt modification on photocatalytic  $\text{O}_2$  evolution to smaller particle sizes (~80 nm on average) and/or improved crystallinity of the resultant  $\text{Ta}_3\text{N}_5$ . Smaller particle sizes allow photoexcited carriers to migrate to surface active sites more readily, and improved crystallinity provides fewer trap sites and thereby more photoexcited carriers for surface reactions. It is thus of interest to clarify how AM salts ( $\text{Na}_2\text{CO}_3$  in particular) alter the morphology and crystallinity of the resulting  $\text{Ta}_3\text{N}_5$ .

Figures 4 and S6(i) show SEM images and XRD patterns of samples at different stages of the nitridation of  $\text{Na}_2\text{CO}_3/\text{Ta}_2\text{O}_5$

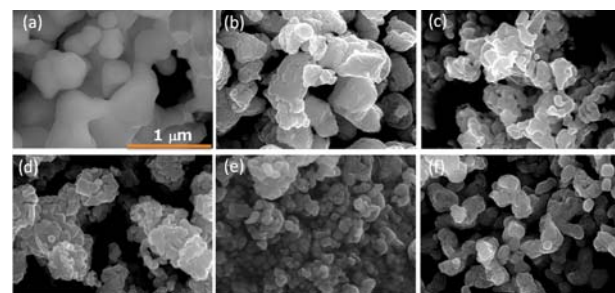


**Figure 4.** SEM images of  $\text{Na}_2\text{CO}_3/\text{Ta}_2\text{O}_5$  (a) before and after nitridation for (b) 1, (c) 5, (d) 10, and (e) 20 h; (f) corresponds to unmodified  $\text{Ta}_2\text{O}_5$  nitrided for 20 h.

into  $\text{Na}_2\text{CO}_3/\text{Ta}_3\text{N}_5$ , respectively. The intermediate  $\text{TaON}$  phase was formed in 1 h of nitridation. Even at this initial stage, the particles began to be miniaturized and exhibit well-defined shapes, although large agglomerated clusters still remained. In contrast, the sample without  $\text{Na}_2\text{CO}_3$  modification did not show any significant reduction in particle size (Figure S7). After 5 h of nitridation, the  $\text{Na}_2\text{CO}_3$ -modified sample exhibited more dispersed particles, which were ~100 nm in size, and the sample showed no sign of the porosity characteristic of  $\text{TaON}$  and  $\text{Ta}_3\text{N}_5$ . Further nitridation of this sample resulted in complete conversion to  $\text{Ta}_3\text{N}_5$  and somewhat smaller particles (~80 nm on average) as a result of the substitution of two  $\text{N}^{3-}$  ions for three  $\text{O}^{2-}$  ions and sintering. It is noteworthy that  $\text{NaTaO}_3$  was formed in addition to  $\text{TaON}$  at the early stage of the nitridation while not being observed in the final product. This suggests that

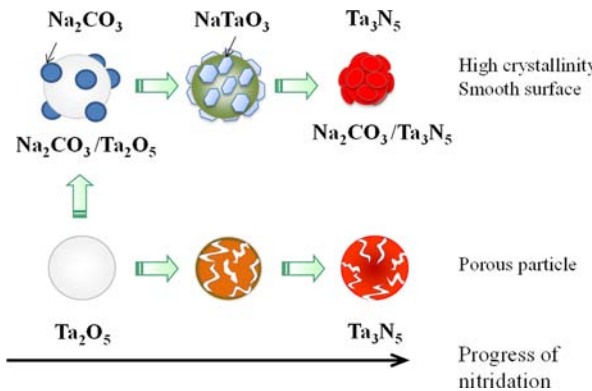


**Figure 5.** Proposed scheme for evolution of conventional  $\text{Ta}_3\text{N}_5$  (bottom) and  $\text{Na}_2\text{CO}_3/\text{Ta}_3\text{N}_5$  (top).

$\text{Na}_2\text{CO}_3$  reacted with  $\text{Ta}_2\text{O}_5$  to form  $\text{NaTaO}_3$  under the present nitridation conditions, and the nucleation of  $\text{NaTaO}_3$  could be responsible for the surface reorganization of  $\text{Na}_2\text{CO}_3/\text{Ta}_2\text{O}_5$  particles upon nitridation. Prolonged nitridation resulted in production of  $\text{Ta}_3\text{N}_5$  without secondary phases because of volatilization of Na species. Transient formation of  $\text{KTaO}_3$  during nitridation of  $\text{K}_2\text{CO}_3/\text{Ta}_2\text{O}_5$  was also confirmed (Figure S6(ii)), attesting the above-mentioned nitridation process. Note that XRD patterns of  $\text{Na}_2\text{CO}_3/\text{Ta}_3\text{N}_5$  with different amounts of  $\text{Na}_2\text{CO}_3$  revealed the presence of  $\text{NaTaO}_3$  at initial Na/Ta ratios higher than 0.2 even after 20 h of nitridation (Figure S8). Evolution of  $\text{NaTaO}_3$  was also previously observed when excessive  $\text{Na}_2\text{CO}_3$  or  $\text{NaCl}$  was added to  $\text{Ta}_2\text{O}_5$  during nitridation.<sup>13a</sup> The use of the small amount of  $\text{Na}_2\text{CO}_3$  was thus essential to prevent formation of residual byproducts while allowing for nucleation of  $\text{NaTaO}_3$  on the surface.

Based on the above results, a proposed development scheme of highly active  $\text{Na}_2\text{CO}_3/\text{Ta}_3\text{N}_5$  photocatalysts can be summarized as illustrated in Figure 5 and the corresponding SEM images (Figure S7). The addition of  $\text{Na}_2\text{CO}_3$  provided dispersed particles of smaller sizes and improved the crystallinity as a result of the nucleation of  $\text{NaTaO}_3$  in the initial stages of nitridation. Further nitridation led to evaporation of Na species and sintering of the anovite-type  $\text{Ta}_3\text{N}_5$ . Some residue could have remained on the surface, without contributing to the activity enhancement. Furthermore, the very small amounts of  $\text{Na}_2\text{CO}_3$  used would not significantly change the semiconducting properties of  $\text{Ta}_3\text{N}_5$ , such as the band gap energy or the flat band potential by acting as dopants, since the amount of Na-species were considerably low.

In summary, the surface loading of AM salts onto  $\text{Ta}_2\text{O}_5$  ( $\text{AM}/\text{Ta} = 0.1$  in molar ratio) was found to be a facile and effective method to improve the water oxidation activity of  $\text{Ta}_3\text{N}_5$ . In particular,  $\text{Na}_2\text{CO}_3/\text{Ta}_3\text{N}_5$  exhibited smaller particles with better crystallinity because of partial dissolution of  $\text{Ta}_2\text{O}_5$  and nucleation of  $\text{NaTaO}_3$  grains. The smaller particle sizes and improved crystallinity are thought to be the principal reasons for the activity enhancement. The present work demonstrates that even a surface modification, such as AM salt loading onto a starting material, can greatly improve the quality and performance of photocatalytic materials, offering a breakthrough in the development of photocatalysts for solar water splitting. Further investigations are in progress to understand the roles of AM salts and relationship between the physicochemical properties and photocatalytic activity.

## ASSOCIATED CONTENT

### Supporting Information

Experimental details and characterization data. This material is available free of charge via the Internet at <http://pubs.acs.org>.

## AUTHOR INFORMATION

### Corresponding Author

domen@chemsys.t.u-tokyo.ac.jp

### Present Address

<sup>†</sup>Department of Chemistry, Graduate School of Science and Engineering, Tokyo Institute of Technology, Japan

### Notes

The authors declare no competing financial interest.

## ACKNOWLEDGMENTS

This work was financially supported by the Grant-in-Aid for Specially Promoted Research (no. 23000009) of the Ministry of Education, Culture, Sports, Science, and Technology (MEXT) of Japan, Advanced Low Carbon Technology Research and Development Program (ALCA) of the Japan Science and Technology Agency (JST), the Global Center of Excellence (GCOE) Program for Chemistry Innovation through Cooperation of Science and Engineering, A3 Foresight Program of the Japan Society for the Promotion of Science (JSPS), PRESTO/JST program, and Nippon Sheet Glass Foundation for Materials Science and Engineering.

## REFERENCES

- (1) (a) Maeda, K.; Domen, K. *J. Phys. Chem. C* **2007**, *111*, 7851. (b) Kudo, A.; Miseki, Y. *Chem. Soc. Rev.* **2009**, *38*, 253. (c) Youngblood, W. J.; Lee, S.-H. A.; Maeda, K.; Mallouk, T. E. *Acc. Chem. Res.* **2009**, *42*, 1966. (d) Maeda, K.; Domen, K. *J. Phys. Chem. Lett.* **2010**, *1*, 2655.
- (2) Hitoki, G.; Ishikawa, A.; Takata, T.; Kondo, J. N.; Hara, M.; Domen, K. *Chem. Lett.* **2002**, *31*, 736.
- (3) Chun, W. J.; Ishikawa, A.; Fujisawa, H.; Takata, T.; Kondo, J. N.; Hara, M.; Kawai, M.; Matsumoto, Y.; Domen, K. *J. Phys. Chem. B* **2003**, *107*, 1798.
- (4) Hara, M.; Hitoki, G.; Takata, T.; Kondo, J. N.; Kobayashi, H.; Domen, K. *Catal. Today* **2003**, *78*, 555.
- (5) Tabata, M.; Maeda, K.; Higashi, M.; Lu, D. L.; Takata, T.; Abe, R.; Domen, K. *Langmuir* **2010**, *26*, 9161.
- (6) Higashi, M.; Domen, K.; Abe, R. *Energy Environ. Sci.* **2011**, *4*, 4138.
- (7) Nakamura, R.; Okamura, T.; Ohashi, N.; Imanishi, A.; Nakato, Y. *J. Am. Chem. Soc.* **2005**, *127*, 12975.
- (8) Silva, C. G.; Bouizi, Y.; Fornes, V.; Garcia, H. *J. Am. Chem. Soc.* **2009**, *131*, 13833.
- (9) (a) Kleiman-Shwarsstein, A.; Huda, M. N.; Walsh, A.; Yan, Y.; Stucky, G. D.; Hu, Y.-S.; Al-Jassim, M. M.; McFarland, E. W. *Chem. Mater.* **2010**, *22*, 510.
- (10) (a) Iwashina, K.; Kudo, A. *J. Am. Chem. Soc.* **2011**, *133*, 13272. (b) Lin, Y.; Xu, Y.; Mayer, M. T.; Simpson, Z. I.; McMahon, G.; Zhou, S.; Wang, D. *J. Am. Chem. Soc.* **2012**, *134*, 5508. (c) Sivula, K.; Zboril, R.; Le Formal, F.; Robert, R.; Weidenkaff, A.; Tucek, J.; Frydrych, J.; Grätzel, M. *J. Am. Chem. Soc.* **2010**, *132*, 7436.
- (11) Kudo, A.; Niishiro, R.; Iwase, A.; Kato, H. *Chem. Phys.* **2007**, *339*, 104.
- (12) Kato, H.; Asakura, K.; Kudo, A. *J. Am. Chem. Soc.* **2003**, *125*, 3082.
- (13) (a) Takata, T.; Lu, D.; Domen, K. *Cryst. Growth Des.* **2011**, *11*, 33. (b) Zhang, F.; Yamakata, A.; Maeda, K.; Moriya, Y.; Takata, T.; Kubota, J.; Teshima, K.; Oishi, S.; Domen, K. *J. Am. Chem. Soc.* **2012**, *134*, 8348.
- (14) Kado, Y.; Lee, C. Y.; Lee, K.; Müller, J.; Moll, M.; Spiecker, E.; Schmuki, P. *Chem. Commun.* **2012**, *48*, 8685.
- (15) Kudo, A.; Omori, K.; Kato, H. *J. Am. Chem. Soc.* **1999**, *121*, 11459.